

## **ENVISAT RADAR ALTIMETRY FOR COASTAL AND INLAND WATERS: CASE-STUDY OF THE COSTA CONCORDIA SHIP TO UNDERSTAND NON- WATER TARGETS USING A TOMOGRAPHIC TECHNIQUE**

Gómez-Enri, J.<sup>1</sup>, Scozzari A.<sup>2</sup>, Soldovieri F.<sup>3</sup>, Vignudelli S.<sup>4</sup>

<sup>1</sup> University of Cadiz (Applied Physics Department), Puerto Real, Spain,

E-mail: [jesus.gomez@uca.es](mailto:jesus.gomez@uca.es)

<sup>2</sup> Consiglio Nazionale delle Ricerche (CNR-ISTI), Pisa, Italy

E-mail: [a.scozzari@isti.cnr.it](mailto:a.scozzari@isti.cnr.it)

<sup>3</sup> Consiglio Nazionale delle Ricerche (CNR-IREA), Naples, Italy,

E-mail: [soldovieri.f@irea.cnr.it](mailto:soldovieri.f@irea.cnr.it)

<sup>4</sup> Consiglio Nazionale delle Ricerche (CNR-IBF), Pisa, Italy,

E-mail: [vignudelli@pi.ibf.cnr.it](mailto:vignudelli@pi.ibf.cnr.it)

### **ABSTRACT**

*Satellite altimetry systems use a nadir-looking radar to sense the water surface, in order to estimate water heights. Non-water targets (e.g. land, ships) are normally treated as contaminants of the pure radar signal reflected by the water surface. Despite the native low resolution of conventional altimetric platforms, there's still the possibility to extract information about eventual land or artificial scatterers inside the antenna footprint, giving the opportunity to better understand how to detect and eventually remove the associated electromagnetic artifacts. In this paper, we use a tomographic technique to retrieve useful information about the location and geometry of such particular targets. We show results from a case-study based on the Costa Concordia cruise ship, which smashed its hull on 13<sup>th</sup> of January 2012 against the coast of Giglio Island, a tiny piece of land in the Tuscan Archipelago (Italy) of the Northwestern Mediterranean. The ship is a strong artificial reflector located off-nadir with respect to the closest Envisat track (orbit 274) to the island. A signature in the Envisat waveforms due to the presence of the Concordia ship is revealed by a change-detection analysis applied to the tomographic reconstruction of the scene observed by the radar. The geometric characteristics of the ship and of the apparent electromagnetic target described in this paper are well compatible with the Concordia ship in its final position. The tomographic technique is therefore a promising tool to make a mapping of targets in coastal and inland waters, and to enhance the possibilities to mitigate such effects when dealing with water height measurements in the presence of such targets.*

**Keywords:** Tomographic reconstruction, Radar Altimetry, RA-2 Envisat, Waveforms, Bright targets, Coastal altimetry, Inland water altimetry.

### **1. INTRODUCTION**

Although designed for open ocean studies, satellite altimetry systems also demonstrated capabilities to monitor the coastal zone and even small inland water bodies, e.g., lakes and rivers [1]. Moreover, satellite altimetry is a technique not only able to detect changes in the water body topography, but it can also provide radar echoes (known as waveforms) that can be processed and transformed into useful information. The enhanced capability of such systems to approach the coastal zone and to study inland waters makes this remote sensing technique an attractive perspective for the study of coastal processes and surface freshwater bodies. In this particular framework, the study of the effect of a steady scatterer is useful to better understand how it interacts with the characteristic response of the water surface.

High rate (18 Hz) echoes are particularly sensitive to non-water targets (e.g., land, ships) that normally are treated as contaminants of the pure radar signal reflected by the water surface. Incidentally, satellite altimetry provides a valuable and unique insight when there are tracks near or above those targets. This is for example the situation that happened on 13<sup>th</sup> of January 2012 when the Costa Concordia cruise ship, with about 4200 passengers onboard, smashed its hull against the coast of Giglio Island, a tiny piece of land in the Tuscan Archipelago of Northwestern Mediterranean (Fig. 1A). Since then, the ship lies partly submerged in the water off the coast of the island. The dual-frequency radar altimeter (RA-2) on-board the Envisat satellite makes one descending pass (orbit 274) near Giglio Island, very close to the accident area (about 2 km), with a revisit time of 30 days (Fig. 1B). This particular condition represents a unique investigation opportunity, given by a steady and relatively large artificial target represented by the Concordia ship, being the orbit in the vicinity of this well-defined reflector, in addition to the pre-existing structure represented by the island.

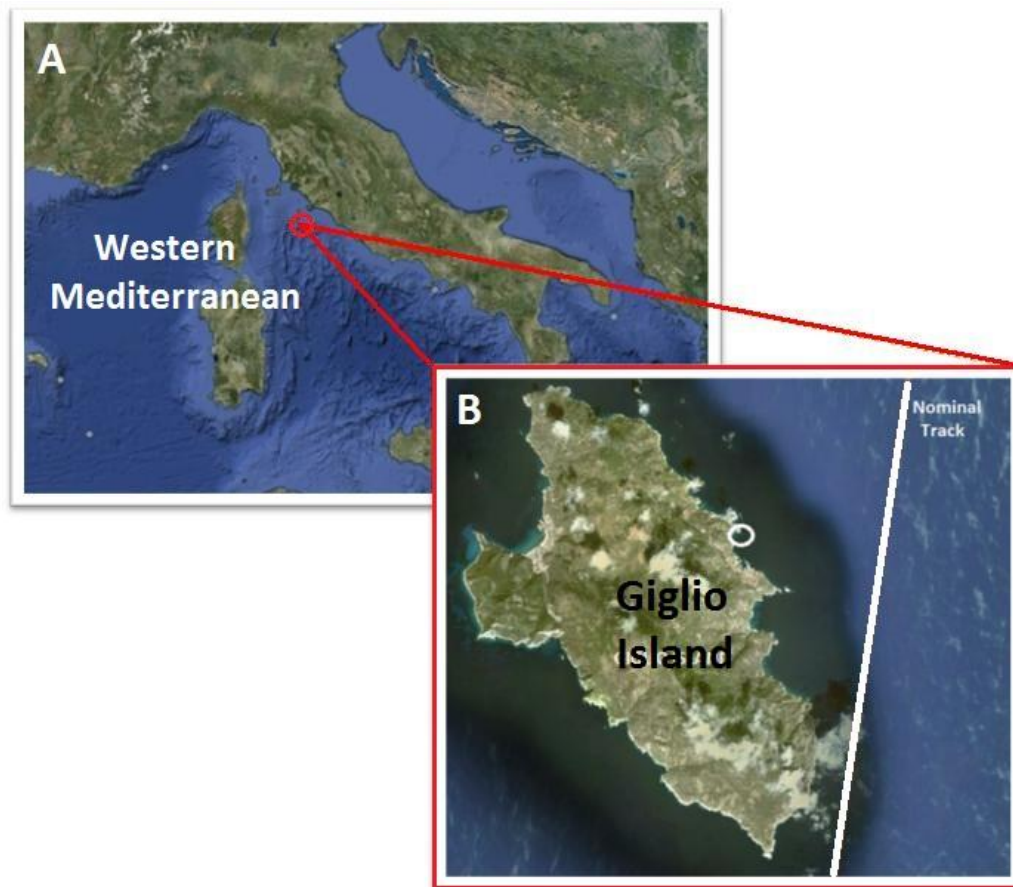


**Fig. 1: Location of the Giglio Island in the Northwestern Mediterranean Sea (red circle in Fig. 1A). The zoom in Fig. 1B shows the nominal track of the RA-2 Envisat satellite (white line) and the exact position of the Concordia ship after the accident (white circle).**

This paper aims at the retrieval of useful information about the location (in terms of height with respect to the sea surface and along-track direction) and extent of the Concordia ship, characterizing its physical and electromagnetic contribution to the background scenario. The ship is a strong artificial reflector (target) located off-nadir with respect to the closest Envisat track (orbit 274) to the island. The electromagnetic anomaly due to the ship is isolated from the background using the tomographic reconstruction approach described in [2]. This can provide additional information for the interpretation of “bright targets” phenomena in the framework of a wider research activity aimed at the extraction of the geophysical information from radar altimetry signals in contaminated contexts. The work is organized as follows: Section 2 shortly describes the tomographic reconstruction technique applied to the radar waveforms. Section 3 introduces the study area. Section 4 illustrates the data sets used: six

descending passes in the new orbit configuration of Envisat. The results obtained from the tomographic reconstruction analysis are provided in section 5. Section 6 contains the conclusions and final remarks.

## 2. THE TOMOGRAPHIC RECONSTRUCTION

This technique belongs to the class of the inverse electromagnetic scattering techniques [3]. For such a class of inverse approaches, the target (i.e., the ship) is accounted for by a contrast function, which identifies the target as an “electromagnetic anomaly” with respect to a background scenario. Here, it is assumed a 2D geometry (2D scans), with the (x-z) plane taken as investigation plane, where the x-axis corresponds to the along-track direction and the z-axis corresponds to the zenith direction. Assuming that the target is located off-nadir, the tomographic reconstruction will be focused on that part of the scan related to the thermal noise, which corresponds to the part of the scan where the scattering targets are above the sea surface.

The contrast function is defined as the relative difference between the equivalent dielectric permittivity of the target (in our case the coastal zone of the Giglio Island and the Concordia ship) and the one of the free space. The contrast function is the unknown part of the problem and is defined as the following a-dimensional quantity:

$$\chi(x', z') = \frac{\varepsilon_{eq}(x', z')}{\varepsilon_0} - 1 \quad (1)$$

Where  $\varepsilon_0$  is the dielectric permittivity of the free space medium, and  $\varepsilon_{eq}(x', z')$  is the (unknown) equivalent permittivity function of the target, given as:

$$\varepsilon_{eq}(x', z') = \varepsilon(x', z') + \frac{\sigma(x', z')}{j\omega} \quad (2)$$

Where,  $j$  is the imaginary unit,  $\omega$  is the angular frequency,  $\varepsilon(x', z')$  and  $\sigma(x', z')$  are the dielectric permittivity and conductivity of the target, respectively. The investigation domain  $D$  within which the contrast function has to be searched for is required in the inversion approach. In our case, the 2D investigation domain is given as a rectangle  $D = [0, 2a] \times [z_{min}, z_{max}]$ ; this means that the extent of the domain  $D$  in the altimeter along-track direction is equal to  $2a$  whereas its height (depth) spans an interval from  $z_{min}$  to  $z_{max}$  that contains the air-sea interface assumed at depth  $z = 0$ . Here, positive/negative  $z$  corresponds to the sea/air domains, respectively. For the tomographic approach, the datum of the problem is given as the field scattered by the reflecting target after a transformation in the frequency domain. Here, we exploit a linear inverse scattering approach that is achieved under a simplified scattering model, known as “Born Approximation” (more information about it can be found in [4]). Under this approximation, a linear integral equation relates the contrast function to the scattered field; the kernel of such an integral equation accounts for the incident field propagating from the altimeter antenna (transmitting) to the target and the trip back from the target to the receiving antenna on the altimeter. The above considerations can be made explicit from a mathematical point of view by writing the integral equation that has to be solved following [4]. This integral equation  $E_s$  is the datum of the problem, i.e., the scattered field collected at a given pulsation and at the spatial location  $(x_s, z_s)$  of the altimeter (working in a monostatic configuration, i.e., the location of the transmitting antenna coincides with the receiving one).

After the discretization of the integral equation  $E_s$ , the problem can be formulated as a matrix inversion problem in the following form:

$$\underline{E}_s = \underline{A}\chi \quad (3)$$

Where  $\underline{A}$  is a matrix arising from the discretization of the integral equation proposed by [4], which is achieved by the method of moments [5];  $\underline{E}_S$  is the stacked data vector made of the  $N \cdot M$  elements, where  $N$  represents the number of spatial points (i.e., the number of waveforms acquired at 18 Hz rate) and  $M$  is the number of working frequencies;  $\underline{\chi}$  represents the discretization of the contrast function (1) in the investigation domain and is represented as a vector made up of the pixellated values of the contrast function in the investigation domain  $D$ . In particular, the investigation domain  $D$  is discretized by rectangular pixels with extent  $\Delta x, \Delta z$  along the  $x$ - and  $z$ -axis respectively. With the aim to counteract the possible ill-conditioning of the inverse problem, the inversion of the matrix relation (3) is performed by means of the Truncated Singular Value Decomposition (TSVD) [6], which is a regularization scheme used to achieve a stable solution; the inversion provides the bi-dimensional spatial map (in the along-track and zenith directions) of the contrast function  $\chi(x', z')$  in the investigation domain  $D$ . Finally, the reconstruction result is given as the modulus of the contrast function, where the regions characterized by a significant modulus are representative of the targets' location and geometry. It is worth noting that the inversion approach works in the frequency domain, thus, a pre-processing step based on a Fourier transform has to be applied to each waveform, in order to perform the inversion of eq. (1) in the transformed domain.

### 3. STUDY AREA

The Giglio Island is one of the islands of the Italian Tuscan Archipelago, located in the Northwestern Mediterranean Sea (Fig. 1). Its territory covers an area of about 24 square km. The coastline is around 27 km long, rich in mineral rocks with intervals of smooth cliffs and bay areas. The inland is predominantly mountainous and almost 90% percent of the surface is covered by Mediterranean vegetation of pine forests and vineyards. Envisat satellite is passing near Giglio Island with one descending pass (orbit 274). The nominal track is about 2 km far the accident area, and this means that the ship falls in the footprint of the radar at any passage following the accident.

### 4. DATA SETS

We analyzed six passes of the Envisat RA-2 covering the period between November 1<sup>st</sup>, 2011 (cycle 108) and March 30<sup>th</sup>, 2012 (cycle 113), extracted from the ESA Sensor Geophysical Data Records (SGDR) product. The collected passes correspond to the new Envisat orbital configuration, which started on October 22<sup>nd</sup>, 2010 with a 30 days repeat cycle. We selected 50 along-track waveforms per cycle at 18 Hz rate. This means that full waveform data are acquired every 0.055 s (about 350 m along track). Each pass (2D scan) used in this study consists of 50 waveforms of consecutively returned along-track signals, selected as the satellite approached the ship. Cycles 108 to 110 correspond to satellite passes before the accident and cycles 111 to 113 correspond to passes later than the accident. Cycle 113 has been the last cycle approaching the Giglio Island before Envisat failure.

For the tomographic reconstruction, the waveforms were organized as a B-scan (an aligned set of in-depth measurements to perform a cross-sectional visualization) with 50 spatial observation points (one per each acquired waveform) spaced by an along-track distance of 350 m. Each waveform is made up of 128 samples with a time step of 3.125 ns, which corresponds to the gate width of the 320 MHz chirp signal of the RA-2 in Ku band. The air-sea interface (also known as *Tracking Point*) is assumed to be at the 47<sup>th</sup> time sample, being the nominal tracking point defined by ESA at gate number 46.5 [7]. Then, each waveform undergoes a Fourier Transform, and the information is arranged in  $M = 21$  uniformly spaced frequencies in the working band [13.4, 13.5] GHz of the radar-altimeter.

The observation domain (i.e., the portion of space where the scattered field is measured) is made up of the 50 spatial observation points, placed at height  $z_s$  (nominal orbit altitude of the altimeter). The investigation domain  $D$ , where to search for the contrast function (representative of the target), has an extent of  $2a = 17150$  m along the  $x$ -axis, which is equal to the one of the observation domain, while along the  $z$ -axis it spans the limited interval  $[z_{min} = -30, z_{max} = 10]$  m. The investigation domain is discretized at a step  $\Delta x = 350$  m,  $\Delta z = 3$  m; in particular, the step along the  $x$ -axis is chosen equal to

the measurement step (observation), whereas the step  $\Delta z$  is comparable with the resolution limits imposed by the working band used in the inversion (put equal to 100 MHz). Inversion of the matrix is carried out by the TSVD scheme, where only the singular values larger than 0.1 times the maximum value are retained in the TSVD expansion.

Finally, we discuss about the spatial resolution attainable with the adopted measurement configuration, which amounts to a height of the measurement configuration of about 800 km and to an extent of the measurement interval of about 17 Km. In this case, the angle of view under which the object is viewed is very small and about  $\theta=0.01$  rad. So, the cross-resolution range, in the case of an optimal sampling of the scattered field, (i.e. the ideal achievable resolution) is about 0.55 m. In the case at hand, the spatial step of the field measurements is about 350m; accordingly, in this case, the associated cross-range resolution is of the same order of the spatial step m, i.e., 350 m. About the range resolution, as well known, this quantity is equal to 3m accordingly to the working band used in the inversion, set to 100 MHz.

## 5. RESULTS

We have investigated the ability of the tomographic reconstruction to retrieve information about the Concordia ship as a target, after the accident. This permits to focus the analysis only on the targets above the sea surface; to make this, we chose only the part of the B-scan in the thermal noise area (gates 4 to 45). Thus, we excluded from the input data to the inversion approach the strong contribution from the air/sea interface. Most of tomographic images reveal the presence of a pattern that extends for some distance along track (Fig. 2).

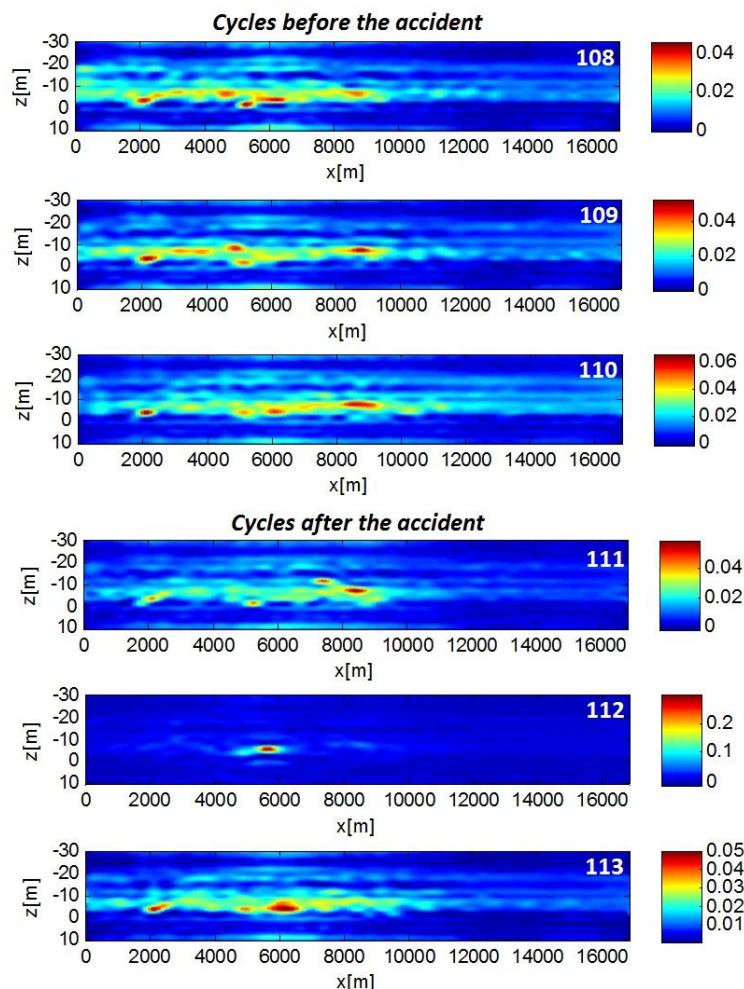


Fig. 2: Tomographic images of the waveforms analyzed along-track cycle by cycle.

The small-scale disturbance due to the ship is overwhelmed by the complex reflection scenario due to the scattering from the island coasts. Therefore, the examination of the simple tomographic reconstructions did not allow detecting in a clear way the Concordia ship.

The presence of the ship, instead, can be assessed by a change detection procedure based on the post-processing of the tomographic images taken just before and after the accident. We chose cycles 109 and 110 before the accident and cycles 111 and 113 after the accident. Cycle 112 was excluded as it appeared strongly different from cycles 111 and 113. Fig. 3A depicts the function defined as:

$$R_1(x_i, z_i) = (|\chi_{113}(x_i, z_i)| - |\chi_{110}(x_i, z_i)|) * (|\chi_{111}(x_i, z_i)| - |\chi_{110}(x_i, z_i)|) \quad (4)$$

Where  $(x_i, z_i)$  spans the investigation domain  $D$  and  $|\chi_k(x_i, z_i)|$  is the modulus of the retrieved contrast functions, where the index  $k$  accounts for the processed cycle. Thus, the function  $R_1(x_i, z_i)$  accounts for the correlation between the two “difference” images after and before the accident. Basically, the area with the maximum value of such correlation represents the common area where the two difference images are significant at the same location. This area is located at about 9000 m along the track and at a height between 5 and 10 m, being the origin of the abscissa located at the first of the 50 observation bins. The upper right panel (Fig. 3B) accounts for the second function defined as the point-by-point difference of the average of the two tomographic reconstructions after the accident and the average of the two reconstructions before the accident:

$$R_2(x_i, z_i) = 0.5 * [(|\chi_{113}(x_i, z_i)| + |\chi_{111}(x_i, z_i)|) - (|\chi_{109}(x_i, z_i)| + |\chi_{110}(x_i, z_i)|)] \quad (5)$$

Also in this case, the function  $R_2(x_i, z_i)$  is maximum in the area around  $x=9000$  m and height between 5 and 10 m. The presence of the height spot, which presumably accounts for the position of the Concordia is quite evident in  $R_3(x_i, z_i)$ , given by:

$$R_3(x_i, z_i) = R_1(x_i, z_i) * R_2(x_i, z_i) \quad (6)$$

The post-processed image is now less affected by artifacts and a clear signature emerges in the area where the ship is located (Fig. 3C). The background parts seem to be efficiently filtered out by the simple change detection technique experimented. It is thus important to check whether this signature is compatible with the presence and location of the ship.

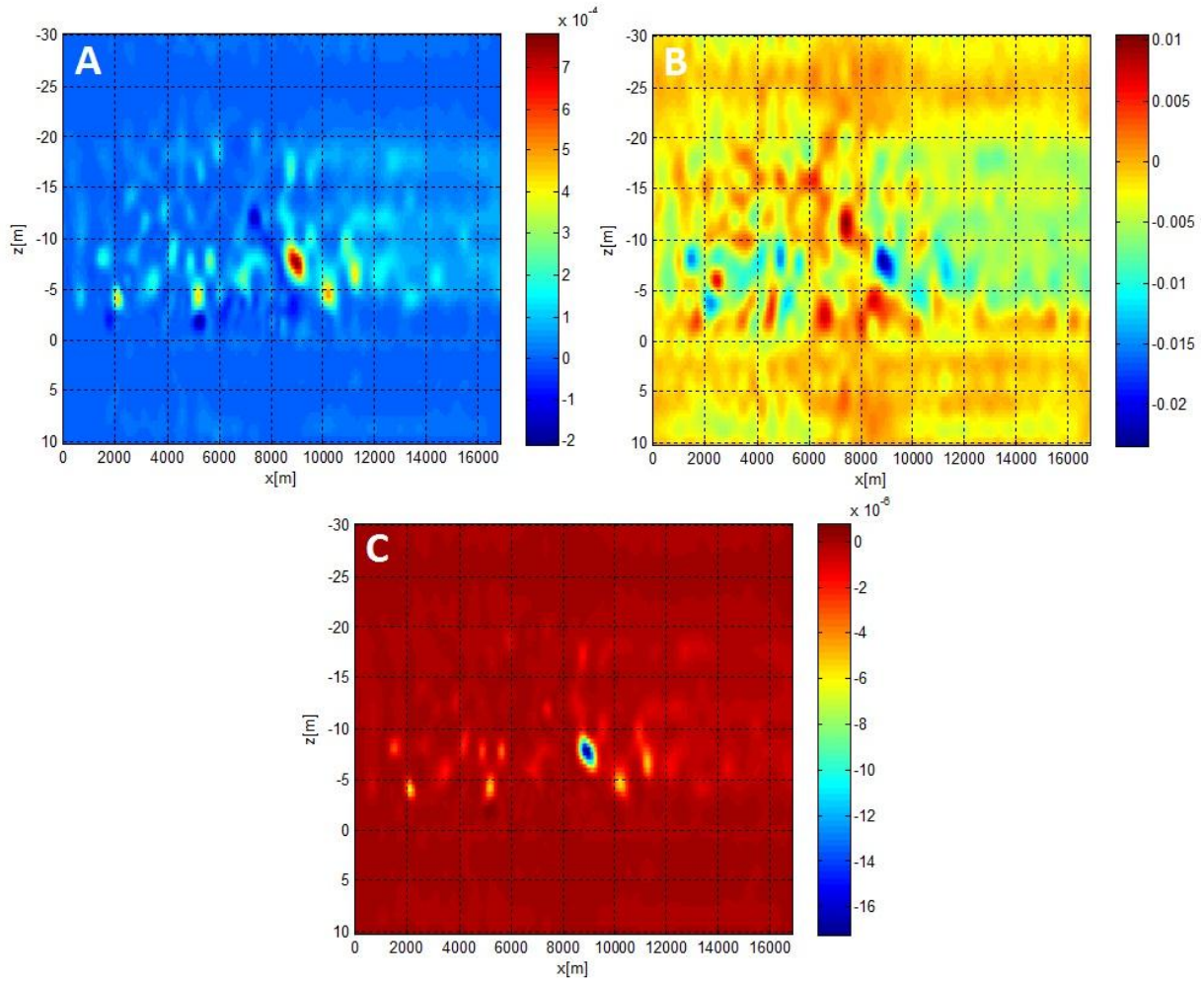


**Fig. 3: Correlation between differences  $(\text{Rec113}-\text{Rec110}) * (\text{Rec111}-\text{Rec110})$  (Fig. 3A). Difference of averages  $(\text{Rec113}+\text{Rec111})/2 - (\text{Rec109}+\text{Rec110})/2$  (Fig. 3B). Element-wise product of the two matrices represented in 3A and 3B (Fig. 3C).**

In order to show that the observed target is compatible with the ship, the main proof is essentially geometric. In fact, it is fundamental to locate the apparent target on the satellite path and check its compatibility with the true position and orientation of the Concordia ship. First of all, the Envisat satellite tracks involved in this study have been plotted together with the route of the ship and its final position. In particular, the apparent target identified in Fig. 3C has been projected on the route pertaining cycle 111, being the closest to the nominal orbit of the satellite (Fig. 4).



**Fig. 4:** Concordia ship route (grey), RA-2 Envisat orbit for cycle 111 (white) and position of the apparent target (red circle). The red line connects the apparent target with the final position of the ship (image from Google maps).

The relationship between the height of a hypothetical point scatterer (over the sea surface) and its off-nadir distance, in order to get a simultaneous echo with the sea surface at nadir, has been calculated. The function plotted in Fig. 5 shows the height of such hypothetical scatterer at the approximate distance between the apparent target and the position of the Concordia (about 2.9 km).

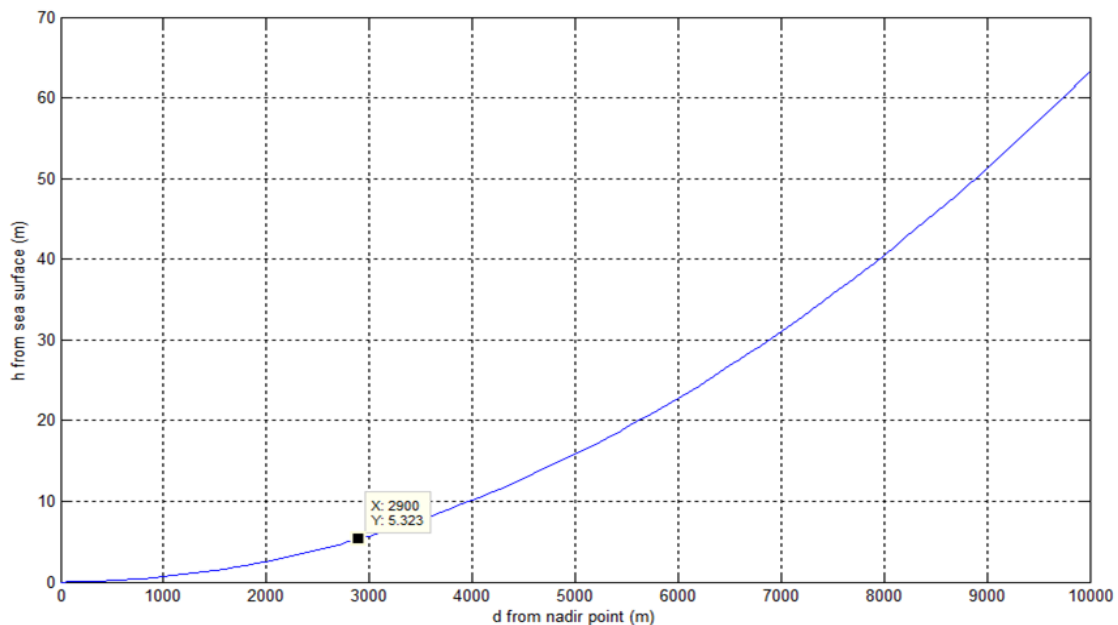


**Fig. 5:** Height over the sea surface of a hypothetical point scatterer vs its off-nadir distance, in order to get a simultaneous echo with the sea surface at nadir

Finally, the height of the ship out of the sea surface has been evaluated, based on a picture taken with an almost front-view, and making proportions with known dimensions of the ship (Fig. 6). The off-sea target identified by the change detection algorithm (Fig. 3C) has an apparent height of about 7 m above the air-sea interface (negative values indicate the target height over the sea, positive values



indicate an undersea depth). Being at an approximate distance of 2.9 km from the nadir projection of the identified signature, a hypothetical scatterer located in the position of the ship should be about 5 m higher than its apparent height (Fig. 5). The expected average height for the identified scatterer (about 12 m) is well compatible with the height out of the sea of the Concordia ship in its final position (about 18 m, Fig. 6). In addition, the fact that such signature is identified with an almost front-view, even if the satellite track passes much closer to the ship, is compatible with the general idea that the apparent target is not associated with the shortest distance to the physical scatterer, but it is associated with the direction that provides the strongest radar return. The intensity of the radar return is highly dependent on the viewing angle, especially for strongly anisotropic and complicated scatterers like the ship is. So, the location of the identified signature inside the wide footprint of the RA-2 radar is not surprising.



Fig. 6: Calculation of the off-sea height of the Concordia ship, based on the proportions between known dimensions.

## 6. SUMMARY AND CONCLUSIONS

A signature in the Envisat waveforms due to the presence of the Concordia ship is revealed by the tomographic analysis enhanced by a simple post-processing step. This is a further proof that small targets emerging from the sea can be detected by satellite altimetry even in complicated contexts, as already shown in the case of icebergs [8]. The tomographic technique is a promising tool to provide a proof of their evidence and would help mapping of targets in coastal and inland waters. The presence of small targets can disturb retracers, i.e., the algorithms that retrieve the geophysical information from the shape of the waveforms. Their identification and removal would permit to clean waveforms data, which can be later treated for the usual altimetry purpose.

The approach can be in principle extended to the detection/evaluation of the variation of the position of a target in two successive passes, only in the case that the target has moved of a distance at least larger than the spatial step (i.e., 350 m). About the possible effect of an additional blurring of the reconstruction due to the movement of the target during the observation time, we can conclude that this is a very residual effect. In fact, by assuming a sample rate of 18 Hz, the target in the “best case” is observed for about 3 sec (50 waveforms/18); this entails that the target should move at speed of  $350\text{m}/3=117$  meters/s to change a position with a related distance larger than the resolution limits, which is not a viable speed for a ship.

## **ACKNOWLEDGMENTS**

SGDR data used in this work were provided by ESA under Category-1 project id: 5785 and COASTALT project (ESA-ESRIN contract 20698/07/I-LG). Acknowledgments go also to the Spanish Ministry of Economy and Competitiveness (project CGL2012-37839) for contributing to the activity.

## **REFERENCES**

- [1]. Vignudelli S., Kostianoy A. G., Cipollini P., Benveniste J. (Editors) (2011), Coastal Altimetry, Springer-Verlag Berlin Heidelberg, doi:10.1007/978-3-642-12796-0, 578 pp.
- [2]. Scozzari A., Gómez-Enri J., Vignudelli S., Soldovieri F. (2012), Understanding target-like signals in coastal altimetry: experimentation of a tomographic imaging technique, *Geophysical Research Letters*, 39, L02602, vol. 239, doi:10.1029/2011GL050237.
- [3]. Colton, D., and R. Kress (1992), *Inverse Acoustic and Electromagnetic Scattering Theory*, Springer, Berlin.
- [4]. Soldovieri, F., and R. Solimene (2010), Ground penetrating radar subsurface imaging of buried objects, in *Radar Technology*, edited by G. Kouemou, pp. 105–126, InTech, Rijeka, Croatia.
- [5]. Harrington, R. F. (1961), *Time-Harmonic Electromagnetic Fields*, McGraw- Hill, New York.
- [6]. Bertero, M. (1989), Linear inverse and ill-posed problems, in *Advances in Electronics and Electron Physics*, vol. 75, edited by P. W. Hawkes, pp. 1–120, Academic, New York.
- [7]. Gommenginger, C., P. Thibaut, L. Fenoglio-Marc, G. D. Quartly, X. Deng, J. Gómez-Enri, P. G. Challenor, and Y. Gao (2011), Retracking altimeter waveforms near the coasts, in *Coastal Altimetry*, edited by S. Vignudelli et al., pp. 61–101, Springer, Berlin, doi:10.1007/978-3-642-12796-0\_4.
- [8]. Tournadre, J., F. Girard-Ardhuin, and B. Legresy (2012), Antarctic icebergs distribution 2002-2010, *J. Geophys. Res.*, doi:10.1029/2011JC007441,